

UC Berkeley

SEMM Reports Series

Title

Shear Lag Analysis of Simple and Continuous T, I, and Box Beams

Permalink

<https://escholarship.org/uc/item/6550h90v>

Authors

Song, Qi-Gen

Scordelis, Alex

Publication Date

1984-06-01

**REPORT NO.
UCB/SESM-84/10**

**STRUCTURAL ENGINEERING AND
STRUCTURAL MECHANICS**

**SHEAR LAG ANALYSIS
OF SIMPLE AND CONTINUOUS
T, I AND BOX BEAMS**

**by
QI-GEN SONG**

A.C. Scordelis, Faculty Investigator

JUNE 1984

**DEPARTMENT OF CIVIL ENGINEERING
UNIVERSITY OF CALIFORNIA
BERKELEY, CALIFORNIA**

**REPORT NO.
UCB/SESM-84/10**

**STRUCTURAL ENGINEERING AND
STRUCTURAL MECHANICS**

**SHEAR LAG ANALYSIS
OF SIMPLE AND CONTINUOUS
T, I AND BOX BEAMS**

**by
QI-GEN SONG**

A.C. Scordelis, Faculty Investigator

JUNE 1984

**DEPARTMENT OF CIVIL ENGINEERING
UNIVERSITY OF CALIFORNIA
BERKELEY, CALIFORNIA**

Abstract

A simplified solution for the shear lag analysis of simple and continuous beams with wide flanges is presented in this investigation. Convergence of the solution and the shear lag effect upon the stress resultants distribution are studied. A computer program, SHLAG, by which the stresses in flanges can be calculated for various load cases, is also described.

Acknowledgements

The author wishes to express his sincere thanks and deepest appreciation to Professor A. C. Scordelis for his encouragement, friendship and instructive discussions.

Gratitude is due also to the staff of the SESM Division for their kind hospitality.

Table of Contents

| | Page |
|---|-------------|
| Abstract and Acknowledgements | i |
| Table of Contents | ii |
| List of Figures | iii |
| Notation | iv |
| 1. Introduction | 1 |
| 2. Solution for Beams with Symmetric Flanges | 1 |
| 3. Solution for Beams with Nonsymmetric Flanges | 4 |
| 4. Fourier Coefficients of Internal Forces | 7 |
| 5. Bending Moment in a Continuous Beam | 7 |
| 6. Convergence Study and Improvement | 10 |
| 6.1 Convergence Study of Loads and Displacements | 10 |
| 6.2 Convergence Study and Improvement of Stresses | 11 |
| 7. Numerical Examples | 17 |
| 7.1 Example 1 - Two-span Continuous Box Girder | 17 |
| 7.2 Example 2 - Cantilever Box Beam under Uniform Load | 22 |
| 7.3 Example 3 - Parameter Study of Single Cell Box Beams | 22 |
| 8. Computer Program SHLAG | 24 |
| 8.1 Input Data | 24 |
| 8.2 Output Data | 26 |
| 9. References | 28 |
| Appendix | 29 |

List of Figures

- Fig. 1 Boundary Conditions**
- Fig. 2 Internal Forces in Web**
- Fig. 3 General Box Beam with Nonsymmetric Flanges**
- Fig. 4 General I Beam with Nonsymmetric Flanges**
- Fig. 5 Continuous Beam**
- Fig. 6 Longitudinal Force Variation in Structure B of Ref. [1]
 at Center Support under Dead Load**
- Fig. 7 Longitudinal Force Variation in Structure B of Ref. [1]
 at Center Support under Prestress Load**
- Fig. 8 Cantilever Beam under Uniform Load**
- Fig. 9 Cross Sections of Box Beam**
- Fig. 10 Loads Considered in Program SHLAG**
- Fig. 11 Sections for Difference NTB**

Notation

(See also Section 8)

$$\alpha = n\pi/l$$

$$\alpha' = (j-n)\pi/l$$

m = integral part of ω , see Eq. (39) and (41)

j = integral part of ω'

$$c(y) = \cosh\alpha y / \cosh\alpha b$$

$$c'(y') = \cosh\alpha y' / \cosh\alpha b'$$

$$\gamma = \frac{(1+\nu)\alpha b - (1-\nu)t}{2 - (1+\nu)\alpha b t}$$

$$\gamma' = \frac{(1+\nu)\alpha b' - (1-\nu)t'}{2 - (1+\nu)\alpha b' t'}$$

$$t = \tanh\alpha b$$

$$t' = \tanh\alpha b'$$

e, e' = distance from center of the web to middle surface of top and bottom flange

d_n = vertical distance from center of web to point of application of longitudinal load,
positive upward

$$\Delta = p_1 q_2 - p_2 q_1$$

$$\omega' = \omega \text{ (for T-beam)}$$

$$\omega' = \frac{\omega}{3} \left(\frac{d}{e+e'} \right)^2 \text{ (for I and box beam)}$$

A, I = Area and moment of inertia of the web

$$R_i = 4bhe^2/I$$

$$R_a = 4bh/A$$

1. Introduction

Stress distribution in wide beam flanges and the related problems of effective width or stress ratio, have been studied for a long time experimentally and also theoretically by harmonic analysis and by finite element analysis [7], [6], [4], [1], [3], [5]. Some problems on this topic, however, still need further investigation.

Since this is basically a stress concentration problem, the convergence or accuracy of the solution is a very important problem to be considered both in harmonic and finite element analyses. Unfortunately, a detailed study of this problem has not been given in the published references.

Based on some rational assumptions for the behavior of the web of the beam, a simplified shear lag analysis for the stresses in the flanges, which is convenient for a wide range of problems is presented in this study. The convergence of the solution for peak stresses in the flanges is studied in detail. It is found that the convergence is not good in some cases and thus an effective technique to improve the convergence and solution is developed.

Theoretically, due to the shear lag effect, the longitudinal distribution of the bending moment in a continuous beam with wide flanges is different from that for a prismatic beam analysed by elementary beam theory. A general procedure for determining the stress resultants in a continuous beam, considering the shear lag effect, is also presented.

Some typical numerical examples are given and the results are compared with the known results by other authors.

The input and output for a computer program, SHLAG, which was written for the shear lag analysis of simple and continuous beams with single cell box section and isolated I- or T-sections is described. This program requires only a minimum amount of input data for the calculation of the stress distribution and the stress ratios in the flanges of these beams for a variety of loading cases.

2. Solution for Beams with Symmetric Flanges

It is assumed that the flange and the web are infinitely flexible out of their own plane and the stresses in the web can be determined by elementary beam theory.

For a simple beam, the stress function in the flange can be taken as

$$\begin{aligned}\phi &= \sum \phi_n \\ \phi_n &= f_n(y) \sin n\pi x/l \\ f_n(y) &= c_1 \cosh \alpha y + c_2 \sinh \alpha y + c_3 \alpha y \cosh \alpha y + c_4 \alpha y \sinh \alpha y\end{aligned}\quad (1)$$

The boundary conditions at the longitudinal edges of the flanges (Fig. 1) are as follows:

a) For I-Beam and T-Beam (Fig. 1a)

at the free edge

$$y=0, \sigma_y=0, \tau_{xy}=0 \quad (2)$$

at the junction of the flange and the web,

$$y=b, \text{ displacement } v=0 \quad (3)$$

and

$$(\epsilon_x)_{flange} = (\epsilon_x)_{web} \quad (4)$$

b) For Box-Beam (Fig. 1b), along the symmetry face,

$$y=0, \tau_{xy}=0, v=0 \quad (5)$$

at the junction

$$y=b, \sigma_y=0, \quad (\epsilon_x)_{flange} = (\epsilon_x)_{web} \quad (6)$$

The total beam bending moment and axial force at any section a distance x from the simple support can be expressed as

$$M = M(x) = \sum_{n=1}^{\infty} m_n \sin \alpha x \quad (7)$$

$$N = N(x) = \sum_{n=1}^{\infty} n_n \sin \alpha x$$

For I-Beam or T-Beam, from conditions (1), (2) and (3) we can obtain:

$$\left. \begin{aligned} \sigma_y &= - \sum_{n=1}^{\infty} A_n c(y) [\alpha y \tanh \alpha y + \gamma (\alpha y - \tanh \alpha y)] \sin \alpha x \\ \sigma_x &= -\sigma_y + 2 \sum_{n=1}^{\infty} A_n c(y) (1 + \gamma \tanh \alpha y) \sin \alpha x \\ \tau_{xy} &= - \sum_{n=1}^{\infty} A_n c(y) [\tanh \alpha y + \alpha y (1 + \gamma \tanh \alpha y)] \cos \alpha x \end{aligned} \right\} \quad (8)$$

For the flange

$$(E \epsilon_x)_{y=b} = \sum_{n=1}^{\infty} A_n \{2 + (1 + \nu) \alpha b t + \gamma [(1 - \nu)t + (1 + \nu)\alpha b]\} \sin \alpha x$$

For the web of a T-Beam (Fig. 2)

$$E \epsilon_x = \left(\frac{1}{A} + \frac{e^2}{I} \right) T - \frac{e}{I} M + \frac{N}{A}$$

T is the total shear transfer from the flange and

$$T = 2 \int_0^x (\tau_{xy})_{y=b} h dx = -2bh \sum_{n=1}^{\infty} A_n (1 + \gamma t + t/ab) \sin \alpha x$$

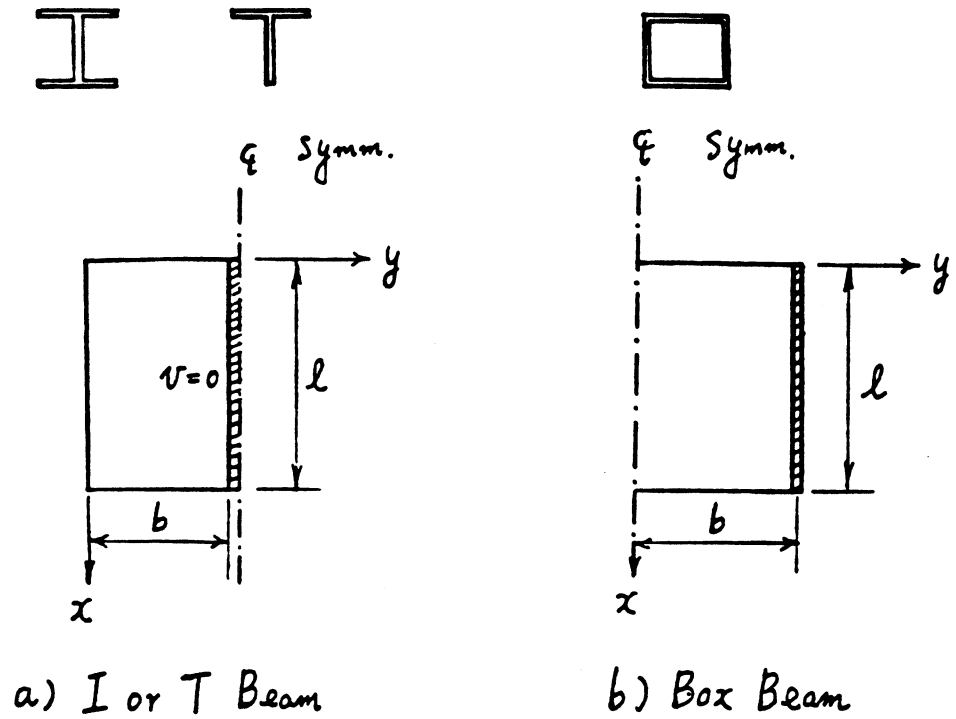


Fig. 1 Boundary Conditions

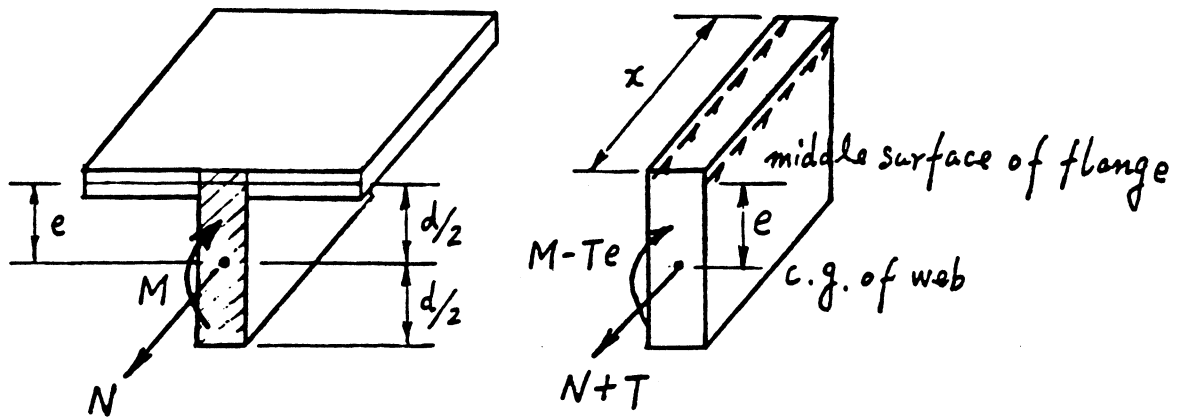


Fig. 2 Internal Forces in Web

Substituting in Eq. (4), we can find

$$\begin{aligned} \{ 2+(1+\nu) \alpha b t+\gamma [(1-\nu) t+(1+\nu) \alpha b] +\left(R_i+R_a\right)\left(1+\gamma t+t / \alpha b\right) / 2\} A_n \\ =-\frac{e}{I} m_n+\frac{n_n}{A} \end{aligned} \quad (9)$$

For I-Beam, similarly,

$$\begin{aligned} \left\{ 2+(1+\nu) \alpha b t+\gamma [(1-\nu) t+(1+\nu) \alpha b]+R_i\left(1+\gamma t+t / \alpha b\right)\right\} A_n=-\frac{e}{I} m_n \\ \left\{ 2+(1+\nu) \alpha b t+\gamma [(1-\nu) t+(1+\nu) \alpha b]+R_a\left(1+\gamma t+t / \alpha b\right)\right\} A_n=\frac{n_n}{A} \end{aligned} \quad (10)$$

For Box-Beam (Fig. 1b) we can obtain

$$\begin{aligned} \sigma_y &= \sum_{n=1}^{\infty} A_n c(y) (\alpha b t - \alpha y \tanh \alpha y) \sin \alpha x \\ \sigma_x &= -\sigma_y + 2 \sum_{n=1}^{\infty} A_n c(y) \sin \alpha x \\ \tau_{xy} &= \sum_{n=1}^{\infty} A_n c(y) [(\alpha b t - 1) \tanh \alpha y - \alpha y] \cos \alpha x \end{aligned} \quad (11)$$

$$\begin{aligned} T &= -bh \sum_{n=1}^{\infty} A_n (1 - t^2 + t / \alpha b) \sin \alpha x \\ \left[2 + \frac{R_i}{2} \left(1 - t^2 + \frac{t}{\alpha b} \right) \right] A_n &= -\frac{e}{I} m_n \\ \left[2 + \frac{R_a}{2} \left(1 - t^2 + \frac{t}{\alpha b} \right) \right] A_n &= \frac{n_n}{A} \end{aligned} \quad (12)$$

3. Solution for Beams with Nonsymmetric Flanges

For a general box beam in which the cross section consists of top, bottom, edge flanges and webs, from the boundary conditions shown in Fig. 3, we can obtain:

$$\begin{aligned} \sigma_x^b &= \sum_{n=1}^{\infty} A_n c(y) (2 - \alpha b t + \alpha y \tanh \alpha y) \sin \alpha x \\ \sigma_x^t &= \sum_{n=1}^{\infty} B_n c(y) [\beta + \eta (2 + \alpha y \tanh \alpha y)] \sin \alpha x \\ \sigma_x^e &= \sum_{n=1}^{\infty} B_n c'(y') [2 + \lambda \alpha y' + (\lambda + \alpha y') \tanh \alpha y'] \sin \alpha x \end{aligned} \quad (13)$$

for bottom, top and edge flanges respectively, where

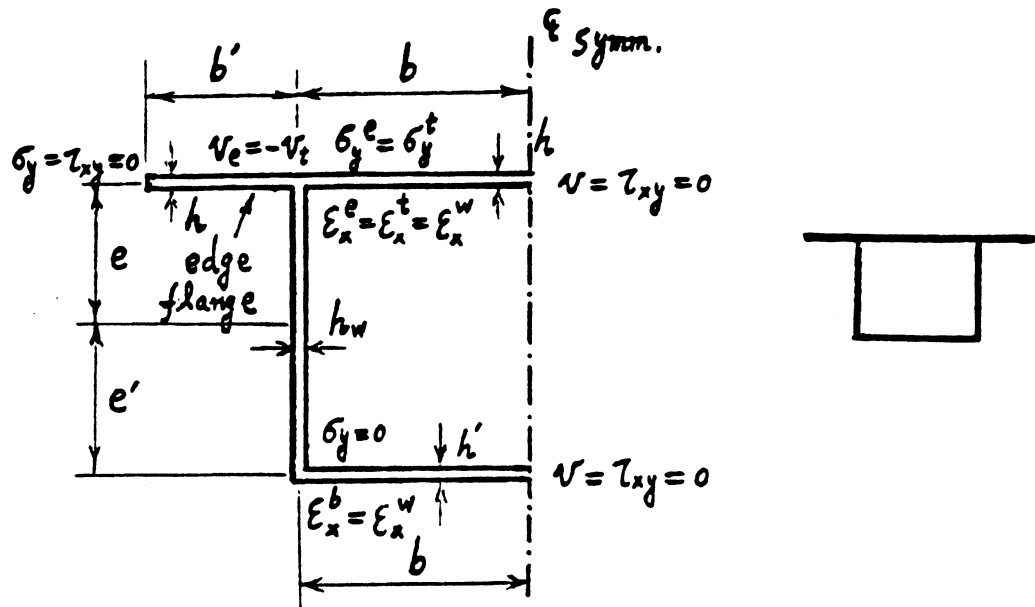


Fig. 3 General Box Beam with Nonsymmetric Flanges

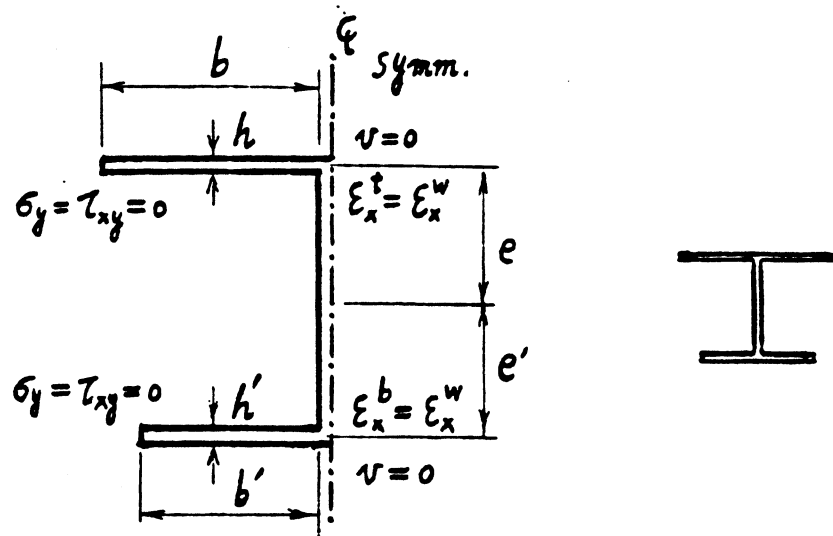


Fig. 4 General I Beam with Nonsymmetric Flanges

$$\left. \begin{aligned} \eta &= 1 + \lambda t' \\ \beta &= \alpha b \left[\lambda \left(\frac{b'}{b} - t t' - \frac{t'}{\alpha b} \right) + \frac{b'}{b} t' - t \right] \\ \lambda &= - \frac{(1+\nu)[\alpha b'(1+t t') + \alpha b(1-t^2)] - (1-\nu)(t+t')}{(1+\nu)[\alpha b'(t+t') + \alpha b t'(1-t^2)] - 2(1+t t')} \end{aligned} \right\} \quad (14)$$

The total shear transfer from the bottom, top and edge flanges are equal to

$$T_b = - \sum_{n=1}^{\infty} A_n f \sin \alpha x \quad (15)$$

$$\left. \begin{aligned} T_t + T_e &= - \sum_{n=1}^{\infty} B_n g \sin \alpha x \\ A_n &= \frac{1}{\Delta} \left[-(e' q_1 + e q_2) \frac{m_n}{I} + (q_2 - q_1) \frac{n_n}{A} \right] \\ B_n &= \frac{1}{\Delta} \left[e' p_1 + e p_2 \right] \frac{m_n}{I} + (p_1 - p_2) \frac{n_n}{A} \end{aligned} \right\} \quad (16)$$

$$\left. \begin{aligned} \Delta &= p_1 q_2 - p_2 q_1 \\ f &= b h' (1 - t^2 + t / \alpha b) \\ g &= b h \left[(\beta + \eta) \frac{t}{\alpha b} + \eta + \frac{t'}{\alpha b} + \frac{b'}{b} (1 + \lambda t') \right] \\ p_1 &= \left(\frac{1}{A} - \frac{e e'}{I} \right) f \\ q_1 &= \left(\frac{1}{A} + \frac{e^2}{I} \right) g + (1 + \nu) \beta + [2 + (1 + \nu) \alpha b t] \eta \\ p_2 &= 2 + \left(\frac{1}{A} + \frac{e'^2}{I} \right) f \\ q_2 &= \left(\frac{1}{A} - \frac{e e'}{I} \right) g \end{aligned} \right\} \quad (17)$$

For an I-Beam or T-Beam, from the boundary conditions shown in Fig. 4 (b' or $h'=0$ for T-beam) we can obtain:

$$\left. \begin{aligned} \sigma_x^b &= \sum_{n=1}^{\infty} A_n c'(y') [2 + (\gamma' + \alpha y') \tanh \alpha y' + \gamma' \alpha y'] \sin \alpha x \\ \sigma_x^t &= \sum_{n=1}^{\infty} B_n c(y) [2 + (\gamma + \alpha y) \tanh \alpha y + \gamma \alpha y] \sin \alpha x \end{aligned} \right\} \quad (18)$$

A_n, B_n have been shown in Eq. (16), but in which:

$$\left. \begin{aligned} p_1 &= \left(\frac{1}{A} - \frac{e e'}{I} \right) f \\ q_1 &= \beta + \left(\frac{1}{A} + \frac{e^2}{I} \right) g \\ p_2 &= \beta' + \left(\frac{1}{A} + \frac{e'^2}{I} \right) f \\ q_2 &= \left(\frac{1}{A} - \frac{e e'}{I} \right) g \end{aligned} \right\} \quad (19)$$

$$\left. \begin{aligned}
 f &= 2b'h'(1+\gamma't'+t'/ab') \\
 g &= 2bh(1+\gamma t+t/ab) \\
 \beta &= 2+(1+\nu)\alpha b t + \gamma [(1-\nu)t+(1+\nu)\alpha b] \\
 \beta' &= 2+(1+\nu)\alpha b't'+\gamma' [(1-\nu)t'+(1+\nu)\alpha b']
 \end{aligned} \right\} (20)$$

4. Fourier Coefficients of Internal Forces

Three elementary loadings are analysed as the basic cases.

a) For a concentrated load P acting at any point $x=\xi$ of a simple beam, the bending moment at any section can be expressed as a Fourier series:

$$M(x) = Pl \sum_{n=1}^{\infty} \frac{2}{n^2 \pi^2} \sin \alpha \xi \sin \alpha x \quad (21)$$

b) For a uniform load w , distributed from $x=a$ to $x=b$, the Fourier series for the bending moment can be obtained by integration of Eq. (21), hence

$$M(x) = 2w l^2 \sum_{n=1}^{\infty} \frac{\sin \alpha x}{n^3 \pi^3} (\cos \alpha a - \cos \alpha b) \quad (22)$$

c) For a pair of longitudinal forces, acting at sections $x=a$ and $x=b$ and at a distance d_n from the center of the web, the axial force and the bending moment at any section are

$$N(x) = N \sum_{n=1}^{\infty} 2(\cos \alpha a - \cos \alpha b) \sin \alpha x / n \pi \quad (23)$$

$$M(x) = -N(x) d_n = -N d_n \sum_{n=1}^{\infty} 2(\cos \alpha a - \cos \alpha b) \sin \alpha x / n \pi \quad (24)$$

All other loading cases can be obtained by superposition of the above three basic loadings.

5. Bending Moment in a Continuous Beam

Unlike a simple beam, the longitudinal distribution of the bending moment in a continuous beam is different depending on whether the shear lag effect is neglected or included.

Including the shear lag effect, the beam can be analysed by the force method in which the $n r$ reactions at the interior supports are adopted as the unknown redundant forces. The bending moment in the web of the basic structure (a simple beam), produced by the external loadings, can be expressed as (Fig. 5):

$$M_p = \sum_{n=1}^{\infty} m_n^o \sin \alpha x$$

Under the unknown reactions $R_1, R_2, \dots, R_k, \dots, R_{nr}$ (Fig. 5), in the web

$$M_r = \sum_{k=1}^{nr} R_k l \sum_{n=1}^{\infty} 2 \sin \alpha x_k \sin \alpha x / n^2 \pi^2$$

can be found by using Eq. (21).

The bending moment in the web, produced by shear transfers from the flanges, can be obtained by using Eq. (15) as:

$$M_f = T_b e' - (T_i + T_e) e = \sum_{n=1}^{\infty} (g e B_n - f e' A_n) \sin \alpha x$$

The corresponding deflections of the basic structure can then be found as:

$$\left. \begin{aligned} EI w_p &= \sum_{n=1}^{\infty} m_n^o l^2 \sin \alpha x / m^2 \pi^2 \\ EI w_r &= \sum_{k=1}^{nr} R_k l^3 \sum_{n=1}^{\infty} 2 \sin \alpha x_k \sin \alpha x / n^4 \pi^4 \\ EI w_f &= \sum_{n=1}^{\infty} l^2 (g e B_n - f e' A_n) \sin \alpha x \end{aligned} \right\} (25)$$

A_n and B_n can be found from Eq. (16) in which the effect of the unknown reactions should be added:

$$A_n = -\frac{e' q_1 + e q_2}{\Delta I} (m_n^o + \sum_{k=1}^{nr} 2 R_k l \sin \alpha x_k / n^2 \pi^2)$$

$$B_n = \frac{e' p_1 + e p_2}{\Delta I} (m_n^o + \sum_{k=1}^{nr} 2 R_k l \sin \alpha x_k / n^2 \pi^2)$$

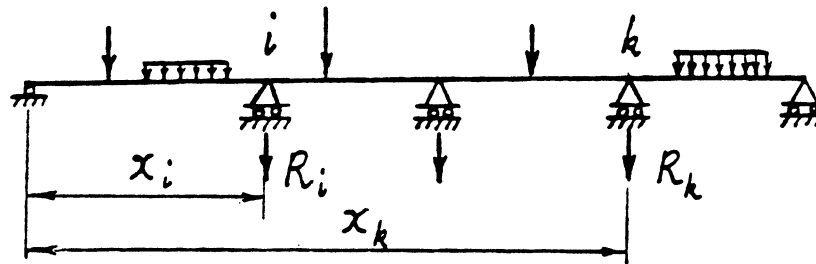
hence,

$$EI w_f = \sum_{n=1}^{\infty} \frac{l^2}{n^2 \pi^2} K_n (m_n^o + \sum_{k=1}^{nr} \frac{2 R_k l}{n^2 \pi^2} \sin \alpha x_k) \sin \alpha x$$

$$K_n = [e g (e' p_1 + e p_2) + e' f (e' q_1 + e q_2)] / \Delta I \quad (26)$$

At the i -th interior support, the final deflection should be equal to zero, hence when $x = x_i$, $w = w_p + w_r + w_f = 0$,

$$\frac{EI}{l^3} \left\{ \sum_{n=1}^{\infty} (1 + K_n) \frac{m_n^o}{n^2 \pi^2 l} \sin \alpha x_i + \sum_{k=1}^{nr} R_k \sum_{n=1}^{\infty} \frac{2(1 + K_n)}{n^4 \pi^4} \sin \alpha x_k \sin \alpha x_i \right\} = 0$$



| x/l | 0.1 | 0.2 | 0.3 | 0.4 | 0.5 |
|-------------------------------------|------|-------------|-------|-------|---------------|
| stress ratio at web-flange junction | .448 | .840 .7* | .944 | 1.025 | 1.198 1.2* |
| effective width b_e/b | 3.49 | 1.383 | 1.121 | .950 | .666 |

* rough values estimated from Fig. 5 of Ref. [3]

Fig. 8 Cantilever Beam under Uniform Load

For all interior supports we can then obtain:

$$\left. \begin{aligned} \sum_{k=1}^{nr} \delta_{ik} R_k &= -\Delta_{ip} \quad (i=1, 2, \dots, nr) \\ \Delta_{ip} &= \frac{l^3}{EI} \sum_{n=1}^{\infty} (1+K_n) \frac{m_n^o}{n^2 \pi^2 l} \sin \alpha x_i \\ \delta_{ik} &= \frac{l^3}{EI} \sum_{n=1}^{\infty} \frac{2(1+K_n)}{n^4 \pi^4} \sin \alpha x_i \sin \alpha x_k \end{aligned} \right\} \quad (27)$$

When longitudinal forces are acting, Eq. (27) can also be used, provided K_n is replaced by

$$H_n = [eg(p_1 - p_2) + e'f(q_1 - q_2)] / \Delta A \quad (28)$$

Eq. (26) to (28) can be used for both Box and I or T beams, provided Eq. (17) and (19), (20) are adopted respectively.

Constants K_n and H_n represent the effect of shear lag. If this effect is neglected, $K_n = H_n = 0$.

For a two-span continuous box beam with equal spans a , some numerical results for the reaction R and the bending moment M_o at the center support for different a/b ratios can be found as shown in Fig. 5.

Neglecting shear lag, $R = 1.25wa$ and $M_o = -.125wa^2$. It can be seen that only for a beam with very small a/b and $1/2bhe^2$, is the shear lag effect upon the bending moment distribution very pronounced. Thus, this effect can be neglected in most practical engineering structures.

6. Convergence Study and Improvement

Because the analytical technique in this study is based on harmonic analysis, it is, therefore, desirable to study the convergence for various cases and its improvement, if necessary.

6.1 Convergence Study of Loads and Displacements

The following conclusions can be made from the numerical results in Tables 1, 2 and 3. For uniform loads, the convergence of series (22) is very good for all points including the discontinuous points of loading. For a concentrated load, the convergence of series (21) is also generally good, although in the vicinity of the concentrated load it is somewhat poor. For the case of a pair of longitudinal forces, however, the convergence of series (23) is not good, especially in the vicinity of the points of application of the forces and also when the two forces acting are close to each other.

In Tables 4 and 5, the redundant reactions are calculated by Eq. (27) and the bending moments are then found by statics. It can be seen that the convergence of series (27) is excellent for calculating the redundant reactions and bending moments. For a two to three span continuous beam, only 11 harmonics are needed for good convergence. For the most critical case of a ten span continuous beam, 21 harmonics are needed.

6.2 Convergence Study and Improvement of Stresses

It can be observed from Eq. (8), (13) and (18) that the series for the stresses in the flanges will converge rapidly when the calculated point is at a short distance from the junction with the web since $c(y)$ decreases very rapidly. The problem of convergence, therefore, will be important and is studied in detail only when $y=b$ in following.

Some ideas of convergence of the stress can be obtained from the numerical results in Tables 6 and 7 for the longitudinal stress ratio at the flange-web junction. The stress ratio is defined as the stress calculated by shear lag theory, divided by the stress at the same point found by elementary beam theory. For a short two-span continuous beam ($l/b=8$) under bending, the error of the stress in the supported section is 1.7% even when the total harmonic number $k = 400$. If the beam is longer, this convergence is poorer. However, at all other sections some distance from the concentrated force, the convergence is very good.

The convergence of stress at the junction of a box beam with symmetric flanges will be studied carefully at first. For the top flange, when $y=b$ Eq. (11) yields:

$$\sigma_t = \sum_{n=1}^{\infty} 2A_n \sin \alpha x \quad (29)$$

When αb is sufficiently large, we can take $t \approx 1$ and from Eq. (12) we can obtain if $n_n = 0$:

$$2A_n = -\frac{e}{I} \frac{m_n}{1 + \omega/n} \quad (30)$$

$$\omega = \frac{he^2 l}{\pi I} \quad (31)$$

It can be seen from Eq. (7), (29) and (30) that at section $x=\xi$, directly under a concentrated load P , the convergence of σ_t is poorer than that of $M(x)$, especially when ω is large. However, it can be improved as follows.

Table 1 $M(x)/w l^2$ by Eq. (22)

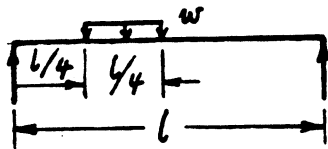
| Loading | x/l No. Harmonic | 1/8 | 1/4 | 3/8 | 1/2 | 3/4 |
|---|-----------------------|---------|---------|---------|---------|---------|
|  | 19 | .019544 | .039064 | .050766 | .046880 | .023432 |
| | 29 | .019535 | .039064 | .050780 | .046875 | .023437 |
| | ∞ | .019531 | .039063 | .050781 | .046875 | .023438 |

Table 2 $M(x)/P l$ by Eq. (21)

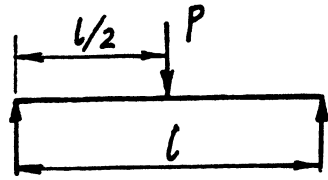
| Loading | x/l No. Harmonic | 0.2 | 0.4 | 0.45 | 0.5 |
|--|-----------------------|--------|--------|--------|--------|
|  | 19 | .09998 | .19980 | .22559 | .24494 |
| | 49 | .10000 | .20002 | .22524 | .24797 |
| | 99 | | | .22501 | .24899 |
| | 199 | | | | .24849 |
| | ∞ | .10000 | .20000 | .22500 | .25000 |

Table 3 $N(x)$ by Eq. (23)

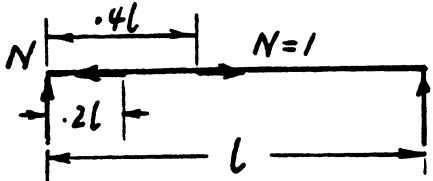
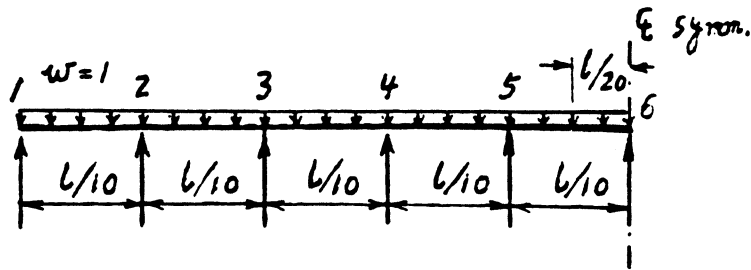
| Loading | x/l No. Harmonic | 0.1 | 0.19 | 0.3 | 0.41 | 0.7 |
|---|-----------------------|---------|--------|--------|--------|--------|
|  | 19 | .02507 | .2805 | .8998 | .2821 | .0051 |
| | 49 | -.01064 | .0634 | 1.0414 | .0634 | -.0021 |
| | 199 | .00537 | -.0838 | .9792 | -.0842 | .0010 |
| | ∞ | 0.0000 | 0.0000 | 1.0000 | 0.0000 | 0.0000 |

Table 4 (total harmonic number = 11) *

| Beam and Loading | l/b | | R_2 | M_2 | M_c |
|------------------|-------|-----|--------|---------|-------|
| | 48 | (1) | 60.006 | -144.07 | 80.61 |
| | | (2) | 60.000 | -144.00 | 80.64 |
| | | (3) | 59.974 | -143.69 | 80.76 |
| | 8 | (1) | 10.001 | -4.002 | 2.239 |
| | | (2) | 10.000 | -4.000 | 2.240 |
| | | (3) | 9.858 | -3.717 | 2.353 |

Table 5 $l/b = 100$ $h/b = 0.05$ *



| No. Harmonic | M_2 | M_3 | M_4 | M_5 | M_6 | M_c | |
|--------------|-------|--------|-------|-------|-------|-------|------|
| (1) | 11 | -11.45 | -7.12 | -8.54 | -8.65 | -7.84 | 4.23 |
| | 21 | -10.63 | -7.70 | -8.48 | -8.25 | -8.34 | 4.20 |
| | 39 | -10.58 | -7.74 | -8.50 | -8.28 | -8.37 | 4.17 |
| (2) | | -10.57 | -7.73 | -8.49 | -8.29 | -8.36 | 4.14 |
| (3) | 39 | -10.49 | -7.76 | -8.47 | -8.28 | -8.33 | 4.19 |

* Results in row (1) and row (3) are computed by Eq. (27) without and with shear lag effect, those in row (2) are computed by ordinary theory.

At section $x = \xi$, from Eq. (21), (29) and (30), we can write:

$$\sigma_t = \sum_{n=1}^k 2A_n \sin \alpha \xi + \Delta \sigma_t^m \quad (32)$$

$$\Delta \sigma_t^m = \sum_{n=k+1}^{\infty} 2A_n \sin \alpha \xi = -\frac{e}{I} \frac{Pl}{\pi^2} S_m \quad (33)$$

where k is a large number and then

$$S_m \approx \sum_{n=k+1}^{\infty} \frac{2 \sin^2 \alpha \xi}{n^2 + \omega n}$$

If ω is replaced approximately by its integral part m , then

$$S_m = \sum_{n=1}^{\infty} \frac{1}{n(n+m)} - \sum_{n=1}^k \frac{1}{n(n+m)} - \sum_{n=k+1}^{\infty} \frac{\cos 2\alpha \xi}{n^2 + nm} \quad (34)$$

in which

$$\sum_{n=1}^{\infty} \frac{1}{n(n+m)} = \begin{cases} \pi^2/6 & (\text{when } m = 0) \\ \frac{1}{m} \left(1 + \frac{1}{2} + \dots + \frac{1}{m}\right) & (\text{when } m > 0) \end{cases}$$

The third term in Eq. (34) converges rapidly and accuracy within 1% can be obtained for S_m using only about 20 terms of this series.

From Tables 6 and 7 it can be observed that the improvement is very effective if Eq. (33) is used.

Under axial forces, the convergence of Eq. (29) is not good for any section, but it can be improved effectively by using Eq. (32) provided $\Delta \sigma_t^m$ is replaced by (see Appendix):

$$\Delta \sigma_t^m = \frac{2N}{\pi} \left(\frac{S_n}{A} + \frac{e}{I} d_n S_{mn} \right) \quad (35)$$

where

$$S_n = \sum_{i=1}^4 \frac{\delta_i}{4} [(\pi - |\beta_i|) \cos j \beta_i + \sin j |\beta_i| \ln 2(1 - \cos \beta_i)] + \sum_{n=1}^j \frac{\cos \alpha' a - \cos \alpha' b}{n} \sin \alpha' x - \sum_{n=1}^k \frac{\cos \alpha a - \cos \alpha b}{j+n} \sin \alpha x \quad (36)$$

j = integral part of ω'

$$\omega' = \frac{\omega}{12} \left(\frac{d}{e} \right)^2$$

$$\beta_1 = (x+a)\pi/l$$

$$\beta_2 = (x-a)\pi/l$$

$$\beta_3 = -(b+x)\pi/l$$

$$\beta_4 = (b-x)\pi/l$$

} (37)

Table 6 Longitudinal Peak Stress Ratios for Simple Beam with Section Shown in Table 4

| case | | concentrated load at midspan (h = .2) | | | axial forces in Table 3 (h = .15) | | |
|------------|----------|---------------------------------------|-----------------|------------|-----------------------------------|-----------------|--|
| <i>l/b</i> | ω | k | <i>x/l</i> = .5 | <i>l/b</i> | k | <i>x/l</i> = .3 | |
| 24 | 37.3 | 39 | 1.098 | 24 | 39 | .842 | |
| | | 99 | 1.136 | | 99 | .929 | |
| | | 400 | 1.163 | | 300 | .977 | |
| | | 39* | 1.180 | | 39* | .963 | |
| | | | | | 99* | .993 | |
| 8 | 12.4 | 39 | 1.420 | 4 | 39 | 1.855 | |
| | | 99 | 1.472 | | 99 | 1.970 | |
| | | 400 | 1.503 | | 300 | 2.024 | |
| | | 39* | 1.521 | | 39* | 2.043 | |
| | | | | | 99* | 2.058 | |

* $\Delta\sigma_t^m$ in Eq. (33) or $\Delta\sigma_t^n$ in Eq. (35) is included.

Table 7 Longitudinal Peak Stress Ratio for Two-span Continuous Beam with Section Shown in Table 4

| case | | uniform load (h = .2) | | | a pair of axial forces at <i>x</i> = .3 <i>l</i> and <i>x</i> = .7 <i>l</i> (h = .15) | | | |
|------------|----------|-----------------------|-----------------|-----------------|---|-----|-----------------|------------------|
| <i>l/b</i> | ω | k | <i>x/l</i> = .5 | <i>x/l</i> = .2 | <i>l/b</i> | k | <i>x/l</i> = .5 | <i>x/l</i> = .35 |
| 48 | 74.3 | 39 | 1.129 | 1.020 | 48 | 39 | .932 | .854 |
| | | 400 | 1.386 | 1.021 | | 99 | .965 | 1.079 |
| | | 2000 | 1.428 | | | 300 | .987 | 1.031 |
| | | 39* | 1.439 | | | 39* | .976 | .951 |
| | | | | | | 99* | .992 | 1.019 |
| 8 | 12.38 | 39 | 2.786 | 1.636 | 8 | 39 | .977 | 1.307 |
| | | 400 | 3.201 | 1.636 | | 99 | 1.034 | 1.610 |
| | | 2000 | 3.257 | | | 300 | 1.061 | 1.550 |
| | | 39* | 3.259 | | | 39* | 1.065 | 1.497 |
| | | | | | | 99* | 1.074 | 1.523 |

* $\Delta\sigma_t^m$ in Eq. (33) or $\Delta\sigma_t^n$ in Eq. (35) is included.

$$\delta_i = \begin{cases} 1 & (\text{when } \beta_i > 0) \\ 0 & (\text{when } \beta_i = 0 \text{ or } \beta_i = 2\pi) \\ -1 & (\text{when } \beta_i < 0) \end{cases}$$

S_{mn} can be calculated by Eq. (36) by replacing j with m .

For T-beam or I-beam with symmetric flanges, similarly:

$$\Delta\sigma_t^m = -\frac{3+\nu}{(3-\nu)(1+\nu)} \frac{e P l}{I \pi^2} S_m \quad (38)$$

$$\Delta\sigma_t^n = \frac{3+\nu}{(3-\nu)(1+\nu)} \frac{2N}{\pi} \left(\frac{S_n}{A} + \frac{e}{I} d_n S_{mn} \right)$$

S_m , S_n and S_{mn} can also be expressed by Eq. (34) and (36), but

$$\left. \begin{aligned} \omega = \omega' &= \frac{4}{(3-\nu)(1+\nu)} \frac{he^2 l}{\pi I} \left(1 + \frac{d^2}{12e^2} \right) && (T\text{-beam}) \\ \omega &= \frac{8}{(3-\nu)(1+\nu)} \frac{he^2 l}{\pi I} && \left. \begin{aligned} & \right\} (\text{symmetric } I\text{-beam}) \\ \omega' &= \frac{\omega}{12} \left(\frac{d}{e} \right)^2 \end{aligned} \right\} \quad (39)$$

For beams with nonsymmetric flanges,

$$\left. \begin{aligned} \Delta\sigma_t^m &= -\frac{e-c}{I} \frac{P l}{\pi^2} S_m \\ \Delta\sigma_b^m &= \frac{e'+c}{I} \frac{P l}{\pi^2} S_m \\ \Delta\sigma_t^n &= \frac{2N}{\pi} \left[\frac{S_n}{A} - (e-c) \frac{c-d_n}{I} S_{mn} \right] \\ \Delta\sigma_b^n &= \frac{2N}{\pi} \left[\frac{S_n}{A} + (e'+c) \frac{c-d_n}{I} S_{mn} \right] \end{aligned} \right\} \quad (40)$$

are used approximately for top and bottom flanges respectively. Eq. (34) and (36) can also be used for S_m , S_n and S_{mn} , but

$$\left. \begin{aligned} \omega &= \frac{1}{2} \frac{l}{\pi I} \left[\left(1 + \frac{b'}{b} \right) h (e-c)^2 + h' (e'+c)^2 \right] && (Box\text{-beam}) \\ \omega &= \frac{4}{(3-\nu)(1+\nu)} \frac{l}{\pi I} \left[h (e-c)^2 + h' \frac{b'}{b} (e'+c)^2 \right] && (I\text{-beam}) \\ \omega' &= \frac{\omega}{3} \left(\frac{d}{e+e'} \right)^2 \end{aligned} \right\} \quad (41)$$

should be used.

It can be concluded that for simple or two to three-span continuous beams, the total harmonic number k may be chosen at 39 and $\Delta\sigma^n$ as well as $\Delta\sigma^m$ may be added if necessary. If the l/b of the beam is very large, k should be greater, for instance, we can take $k=l/b$ and the calculation work will be increased considerably. Fortunately, if a/b (a = length of the span) is very large, the value of k is not important, because in this case the shear lag effect is negligible.

Finally, some remarks regarding the assumptions for the web, which in this study has been analysed by elementary beam theory. When $\alpha d = n\pi d/l$ is very large, beam theory is no longer accurate. If the web is analysed by the theory of elasticity, then under an antisymmetric vertical loading about web mid depth, Eq. (12) should be replaced by

$$\left\{ 1 + \frac{h}{h_w} \frac{(\cosh \alpha d - 1)[t + (1-t^2)\alpha b]}{2(\sinh \alpha d - \alpha d)} \right\} A_n = \left(\frac{1+\nu}{2} - \frac{\sinh \alpha d}{\sinh \alpha d - \alpha d} \right) \frac{p_n}{h_w} \quad (42)$$

where p_n is the Fourier coefficient of the distributed load.

When $\alpha d \rightarrow 0$, Eq. (42) will be identical with Eq. (12). When αd and αb are sufficiently large, then

$$\left(1 + \frac{h}{h_w} \right) A_n = - \frac{1-\nu}{2} \frac{p_n}{h_w} \quad (43)$$

This is essentially different from Eq. (30).

7. Numerical Examples

7.1 Example 1 - Two Span Continuous Box Girder Bridge, Ref. [1]

A two span continuous box girder, Structure B in Ref. [1], was analysed by the computer program SHLAG (total harmonic number $k=100$, as in Ref. [1]) of this study. The longitudinal membrane forces in the flanges are plotted and compared with those of Ref. [1] in Figs. 6 and 7.

From Fig. 6 we can observe:

1. The two analytical results agree well except at the junction point b and t, where N_t and N_b of SHLAG are somewhat greater than those of Ref. [1] because in SHLAG, $\Delta\sigma^m$ of Eq. (32) has been accounted for. It can be expected that if a greater number for k is used in Ref. [1], these two results will be closer.
2. The lower estimate of the peak stresses in Ref. [1] results in the total internal bending moment (24670 kip-ft) in Ref. [1] being smaller than the correct one (25453 kip-ft) and the moments contributed by the stresses in the flanges are also smaller than those found by SHLAG (see the comparison in Fig. 6).
3. In SHLAG, it is assumed that the web is infinitely flexible out of its own plane and it is considered as a beam on the vertical plane. The other small discrepancy of the above two results may be produced by this approximate assumption.

For the case of prestress load (Fig. 7), a similar observation can be obtained.

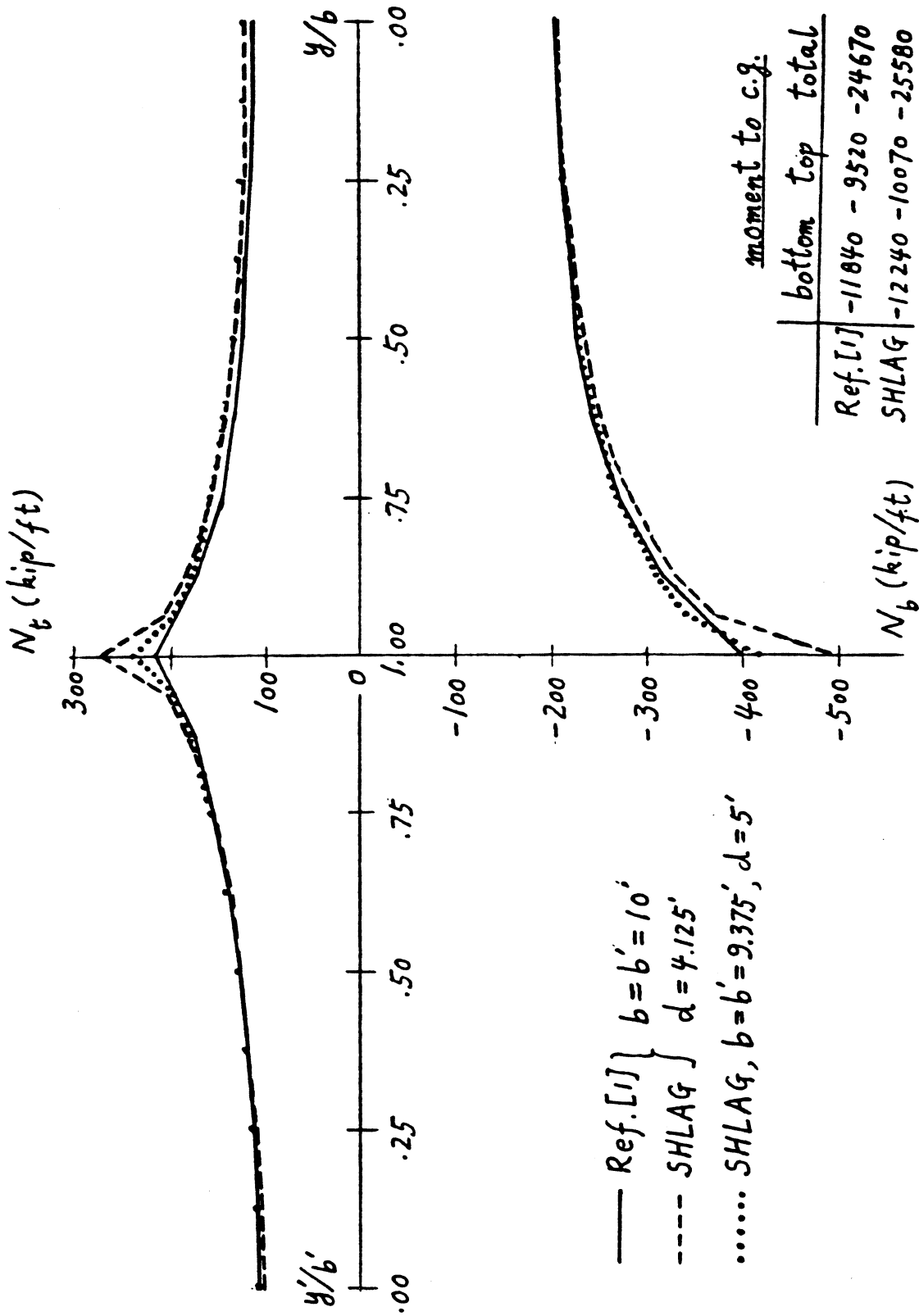


Fig. 6 Longitudinal Force Variation in Structures B of Ref. [1] at Center Support under Dead Load

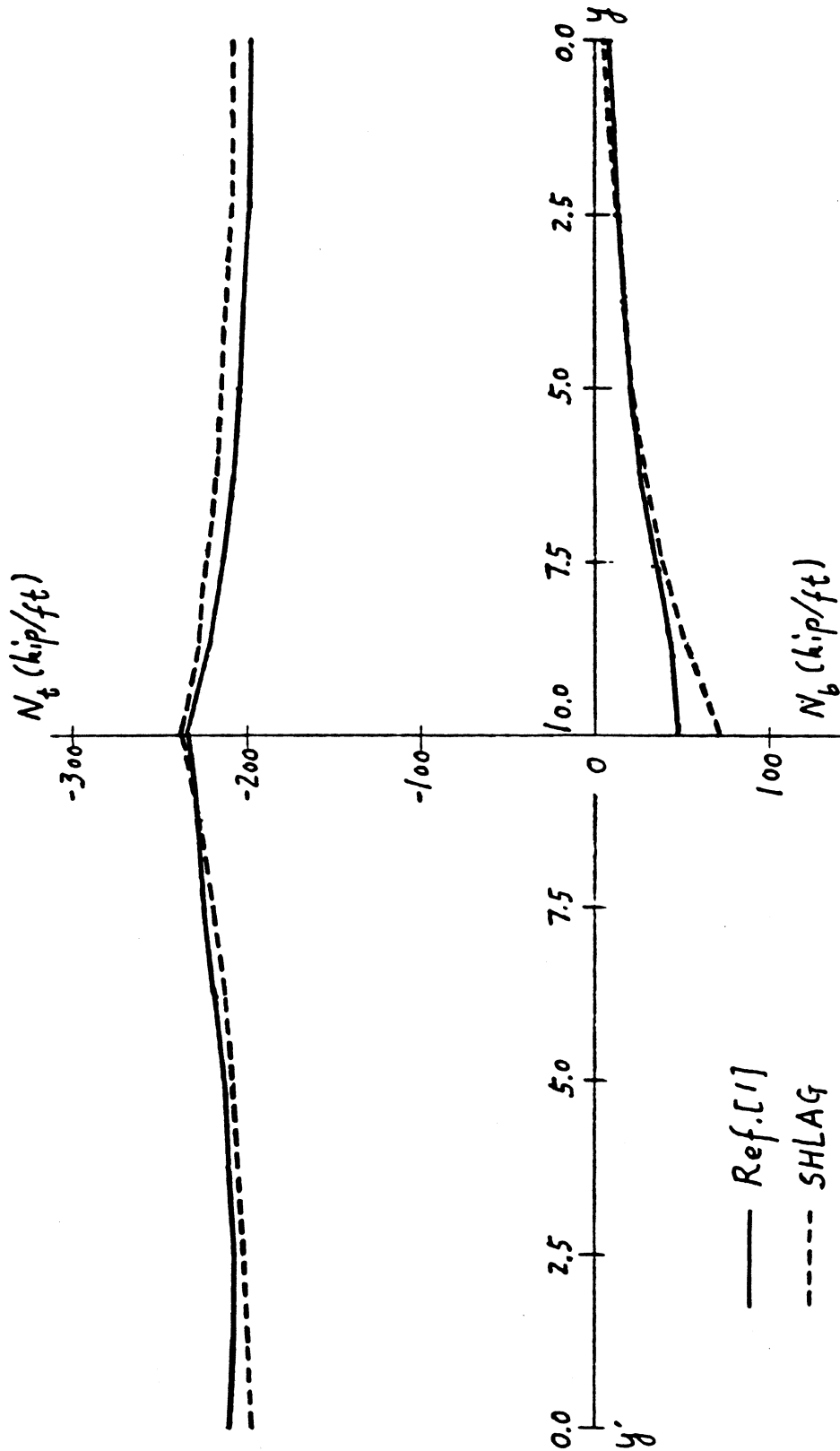
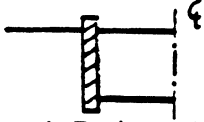
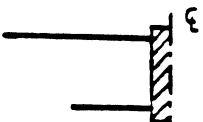
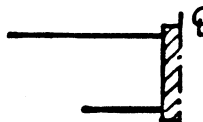
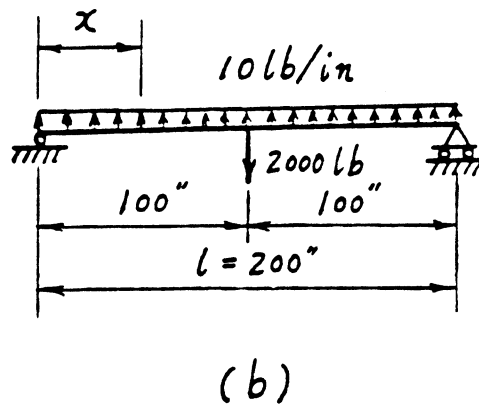
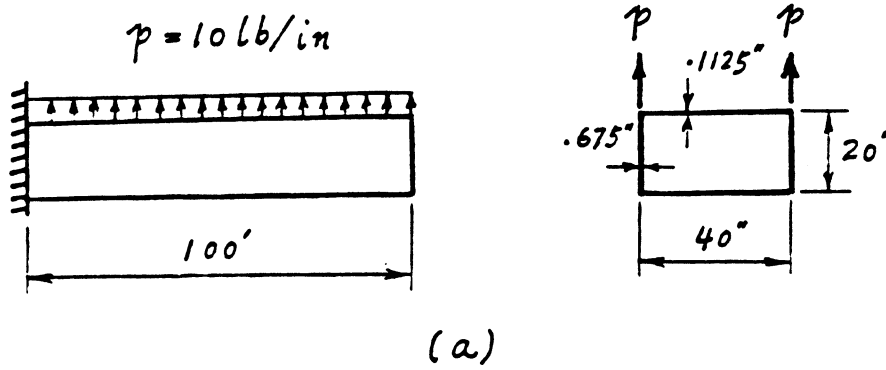


Fig. 7 Longitudinal Force Variation in Structure B of Ref. [1] at Center Support under Prestress Load

Table 8 Stress Ratio in Bottom Flange of Structure B of Ref. [1] and Its Equivalent I-Beam

| distance from web edge |  Poisson's Ratio $\nu=.15$ |  $\nu=.15$ |  $\nu=0$ |
|------------------------|--|---|--|
| 0 | 1.534 | 1.539 | 1.525 |
| | 1.384* | 1.383* | 1.371* |
| .586 | 1.243 | 1.255 | 1.247 |
| 1.172 | 1.139 | 1.159 | 1.154 |
| 1.758 | 1.060 | 1.085 | 1.082 |
| 2.344 | .999 | 1.025 | 1.025 |
| 2.930 | .950 | .977 | .979 |
| 3.516 | .911 | .936 | .940 |
| 4.102 | .878 | .902 | .908 |
| 4.688 | .851 | .873 | .881 |
| 5.273 | .829 | .848 | .858 |
| 5.859 | .811 | .826 | .838 |
| 6.445 | .796 | .807 | .822 |
| 7.031 | .784 | .791 | .808 |
| 7.617 | .775 | .776 | .796 |
| 8.203 | .769 | .763 | .786 |
| 8.789 | .765 | .751 | .777 |
| 9.375 | .764 | .740 | .769 |

* $\Delta\sigma^m$ in Eq. (32) is ignored.



| x/l | 0.1 | 0.2 | 0.3 | 0.4 | 0.5 |
|-------------------------------------|------|-------|-------|-------|-------|
| stress ratio at web-flange junction | .448 | .840 | .944 | 1.025 | 1.198 |
| effective width b_e/b | 3.49 | 1.383 | 1.121 | .950 | .666 |

* rough values estimated from Fig. 5 of Ref. [3]

Fig. 8 Cantilever Beam under Uniform Load

For comparison, the bottom flange stress ratios for the box girder of Structure B in Ref. [1] and for an equivalent I-beam are analysed by SHLAG for dead load. The latter section is obtained by joining together the two webs of the former section. From the results in Table 8 it can be concluded that the stress distributions in the bottom flange are almost the same for the two sections. Also the effect of Poisson's ratio is negligible as can be seen by comparing the results in the last two columns.

7.2 Example 2 - Cantilever Box Beam under Uniform Load

A symmetrical cantilever tube in Ref. [3] (Fig. 8a) can be replaced by an equivalent simple beam (Fig. 8b). The calculated results by SHLAG are compared with those of Ref. [3] in Fig. 8.

It can be seen that the results by SHLAG agree qualitatively with those in [3] and in a certain zone the effective width is greater than b and the stress ratio is smaller than 1 as pointed out in Ref. [3].

7.3 Example 3 - Parameter Study of Single Cell Box Beam

Computer analyses of some single cell box beams with different spans and various cross sections shown in Fig. 9 were performed using the SHLAG program. From the results in Table 9, we can conclude:

1. The shear lag effects at a section located under a concentrated force are much more pronounced than those at other sections.
2. The stress ratios at point b and t (Fig. 9) at the interior support sections of a continuous beam are much greater than those at a section just under a concentrated load on a simple beam with the same dimensions.
3. As pointed out by many authors, an increase of the ratio a/b (a =span) results in a decrease in the stress ratio.
4. Under uniform load, the stress ratios at the interior support section of a two span continuous beam are somewhat smaller than those for a ten-span beam with the same span. The intermediate spans of a ten-span continuous beam can be approximated by a fixed-end beam.
5. In a ten-span continuous beam under uniform load, it can be seen from Table 9 that the stress ratio at the support sections $x/l=0.2$ and 0.4 , where the bending moments are smaller, are greater than those at other support sections.
6. The stress ratios for sections 1, 2 and 3 at point b are quite similar, but at point t they are somewhat different.

Table 9 Ratio of σ_x under Uniform Load

| a (Span Length) | Beam Type | Cross Section | x/l x = Dist. from Left Supp. | Ratio of σ_x | | $\frac{M}{w a^2}$ |
|-----------------------|---------------------------------------|------------------|---------------------------------------|---------------------|------------|-------------------|
| | | | | point b | point t | |
| 24 | Simple * | 2 | .5 | 1.180 | 1.155 | |
| | Two- span Continu. | 1 | .5 | 1.439 | 1.439 | -.1250 |
| | | 2 | .2 | 1.021 | 1.021 | .070 |
| | Ten- span Continu. (Table 5) | 2 | .5 | 1.422 | 1.352 | -.1250 |
| | | | .2 | 1.109 | 1.017 | .070 |
| | | | .1 | 1.473 | 1.421 | -.1056 |
| | | | .2 | 1.550 | 1.490 | -.0774 |
| | | | .3 | 1.525 | 1.467 | -.0851 |
| | | | .4 | 1.533 | 1.474 | -.0828 |
| | Two-Span Continu. | 3 | .5 | 1.530 | 1.471 | -.0837 |
| .45 | | | 1.028 | 1.023 | .0418 | |
| 4 | Two- span Continu. | 1 | .5 | 1.432 | 1.532 | -.1250 |
| | | | .2 | 1.021 | 1.025 | .070 |
| | | 2 | .5 | 3.259 | 3.259 | |
| | | | .2 | 1.636 | 1.636 | |
| | | 3 | .5 | 3.167 | 2.805 | |
| | | | .2 | 1.616 | 1.470 | |
| | | .5 | 3.149 | 3.828 | | |
| | | .2 | 1.628 | 1.726 | | |

* under a concentrated load at $x=0.5l$.

8. Computer Program SHLAG

In the program, the distribution of longitudinal stress σ_x and "Stress Ratio" in flanges of a simple and multiple-span continuous beam with Box, I or T shape cross section can be computed for various loadings (Fig. 10). The "Stress Ratio" at a point is defined as the ratio of the stresses calculated with and without considering the shear lag effect. The latter stress is given by elementary beam theory. For a continuous beam, the redundant reactions can be determined with and without considering the shear lag effect. The various loadings can be obtained by superposition of three basic loadings:

- a) a concentrated load of any magnitude and acting at any point.
- b) a uniform load of any intensity and distributed over any length of the beam.
- c) a pair of equal and opposite longitudinal forces acting at any point of any two sections.

8.1 Input Data

SHLAG was written for the micro-computer, CP/M2 for TRS-80 Model II. All input data can be read from the console directly.

1. Title (20 A 4) - 1 line

Title of the problem to be printed with output

2. Control data (9 I 6) - 1 line

- k Total harmonic number to be used (≤ 300)
- nx Number of prescribed cross sections at which results are required except for the intermediate supported sections which have been chosen as prescribed sections automatically (≤ 40)
- ny Number of points for calculation, located at equal transverse distances, in bottom, top and edge flange of each prescribed section (>1)
- nr Number of redundant reactions (≤ 10)
- n/ Number of concentrated loads (≤ 20)
- nw Number of uniform loads (≤ 20)
- nn Number of pairs of longitudinal loads (≤ 20)
- ntb Type number of beam. For box beam, $ntb=0$ or 1 (Fig. 11). For I and T beams, $ntb=2$ and 3

3. Geometry data (8 F 12.5) - 1 line

- l Total overall beam length
- h Thickness of top and edge flange
- h' Thickness of bottom flange
- h_w Thickness of web
- b Half width of top flange see Fig. 11
- b' Half width of bottom or edge flange
- d Depth of beam
- ν Poisson's ratio

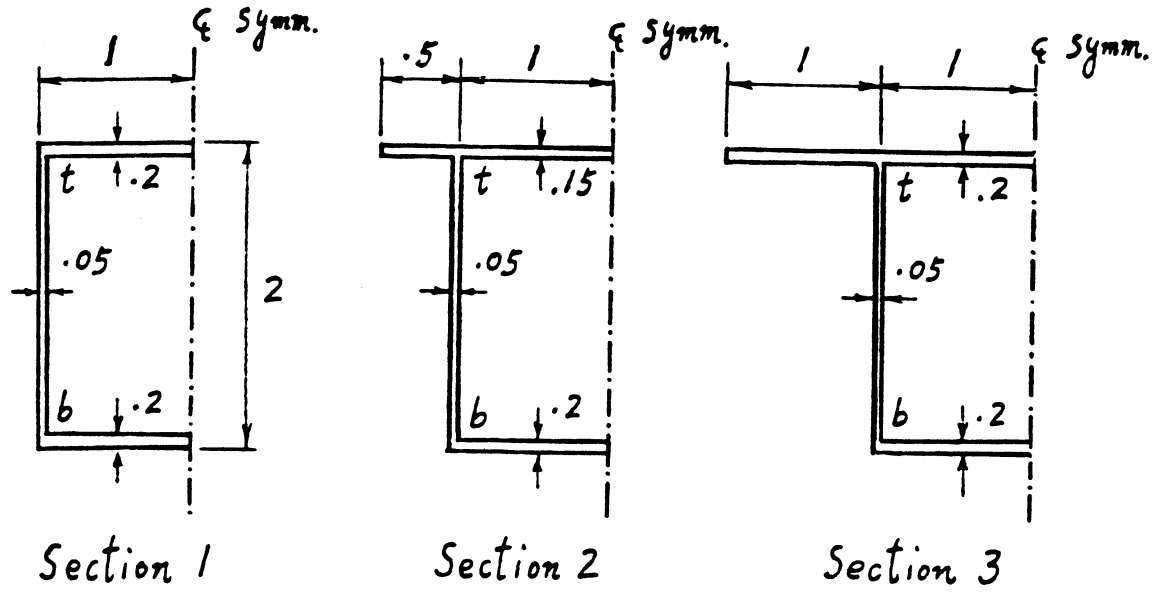


Fig. 9 Cross Sections of Box Beam

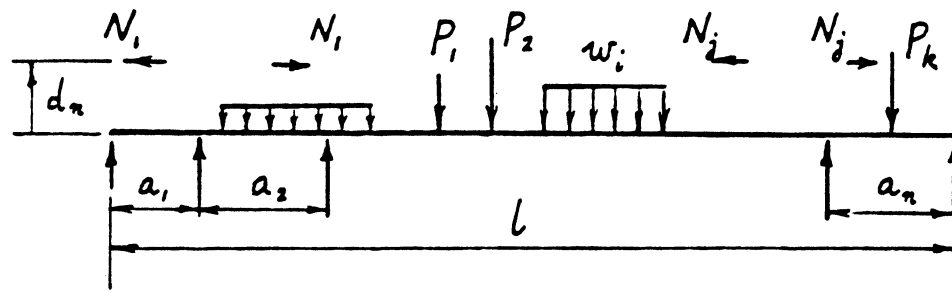


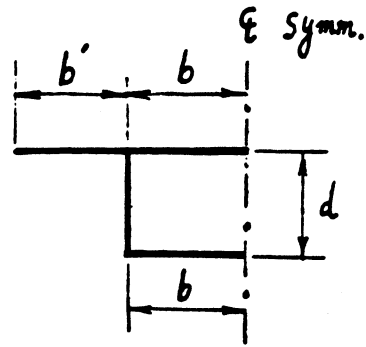
Fig. 10 Loads Considered in Program SHLAG

4. $xx(1), xx(2), \dots, xx(nx)$ - x-coordinates of prescribed sections at which results are required except supported sections (6 F 16.8).
Data in one line cannot exceed 6.
Use as many lines as necessary.
In the following, items 5-7 are used for applied loads. Loads per one web are used for input. Items 8-9 are needed for continuous beam only.
5. **Concentrated load data** (2 F 16.8) - 1 line for each load
 $pv(i)$ Magnitude of the i-th concentrated load
 $pl(i)$ x-coordinate of the i-th load
 $i=1, 2, \dots, n/$, are needed only when $n/ \neq 0$.
6. **Uniform load data** (3 F 16.8) - 1 line for each load
 $ul(i,1)$ Intensity of the i-th uniform load
 $ul(i,2)$ x-coordinate of left end of load
 $ul(i,3)$ x-coordinate of right end of load
 $i=1, 2, \dots, nw$, are needed only when $nw \neq 0$.
7. **Longitudinal load data** (4 F 16.8) - 1 line for each pair of loads
 $af(i,1)$ Magnitude of the i-th pair of longitudinal loads
 $af(i,2)$ x-coordinate of point of application of left load
 $af(i,3)$ x-coordinate of point of application of right load
 $af(i,4)$ Vertical distance from web center to point of application of load, positive upward.
 $i=1,2, \dots, nn$, are needed only when $nn \neq 0$.
8. **mm** harmonic number for calculating displacement (I6) - 1 line
9. **Intermediate interior supports data** (6 F 16.8) - data in one line cannot exceed 6. Use as many lines as necessary.
 $xr(i)$ x-coordinates of the i-th intermediate interior support.

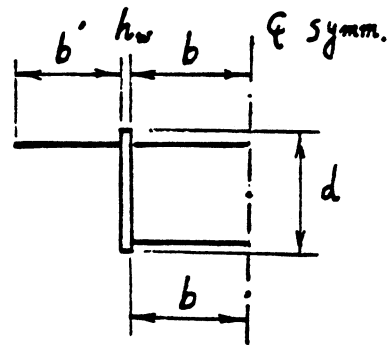
8.2 Output Data

1. All input data are written according to the input order for checking
2. $R_I = bhe^2/I$
FT/M, FB/M = Beam theory stress coefficient for top and bottom flange
 c = Distance from web center to centroid of total cross section, positive upward
TA, TI = Area, moment of inertia of total cross section
3. ω (See Eq. (41), (39))
4. R_o = Intermediate reactions calculated without considering shear lag effect
5. R = Intermediate reactions calculated with considering shear lag effect
6. x/L = Relative x-coordinates of prescribed sections
7. MB, MS = Total bending moment at section x, calculated without and with considering shear lag effect
N = Total axial force at section x
BSB, BST = Beam theory stress in bottom and top flange at section x

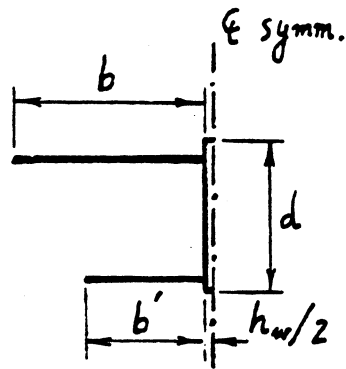
$NTB = 1$
(All center line dimension)



$NTB = 2$
(Center line dimension
for flange only)



$NTB = 2$



$NTB = 3$

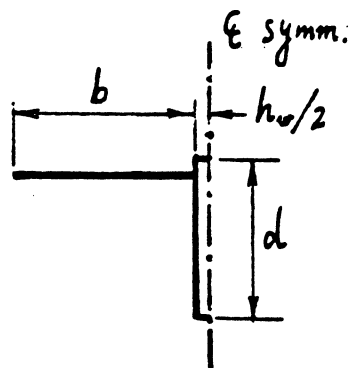


Fig. 11 Sections for Different NTB

8. Y, YP = y, y' - coordinates of points at which stress is computed
SST//RST = Shear lag stress and stress ratio of top flange at point with coordinate (x,y)
SSB//RSB = Shear lag stress and stress ratio of bottom flange at point with coordinate (x,y) for box beam or with coordinate (x, y') for I beam
SSE//RSE = Shear lag stress and stress ratio of edge flange at point with coordinate (x, y')

At point (x,b) and (x, b'), where peak stresses occur, the stresses and stress ratio are printed three times. First, $\Delta\sigma^m$ and $\Delta\sigma^n$ of Eq. (33) and (35) are not included. Second, $\Delta\sigma^n$ is included. Third, both $\Delta\sigma^n$ and $\Delta\sigma^m$ are included.

Items 6-8 are printed repeatedly for each prescribed section.

9. References

1. "Precast Segmental Box Girder Bridge Manual", Post-Tensioning Institute and Prestressed Concrete Institute, 1978, pp. 44-49.
2. I.M. Ryshik and I.S. Gradstein, "Tables of Series, Products, and Integrals", Ver Deutscher Verlag der Wissenschaften, Berlin, 1957, p. 37.
3. Douglas A. Foutch and P.C. Chang, "A Shear Lag Anomaly", Journal of the Structural Division, ASCE, Vol. 108, July, 1982, pp. 1653-1658.
4. G.M. Sabnis and W.D. Lord, "Investigation of the Effective Width of Reinforced Concrete T-Beam", Preprint 2746, ASCE Annual Convention and Exposition, Philadelphia, PA, September 27 - October 1, 1976.
5. Kurt K.J. Irrcher, "The Effective Flange Width of Typical Prestressed Concrete T-Beams under Service Conditions", M.S. Thesis, Department of Civil Engineering, University of Calgary, May, 1983.
6. Brendal, G., "Strength of the Compression Slab of T-Beams Subject to Simple Bending", ACI Journal, January, 1964, pp. 57-76.
7. Winter, G., "Stress Distribution in and Equivalent Width of Flanges of Wide Thin-Wall Steel Beams", Technical Note No. 784, National Advisory Committee for Aeronautics, Nov. 1940.

Appendix

When $m_n=0$ and $y=b$, from Eq. (10), (12) and (23) we can obtain:

$$\Delta\sigma_b^n = \frac{1}{A} \sum_{n=k+1}^{\infty} \frac{n_n}{1+\omega'/n} \approx \frac{2N}{\pi A} S_n \quad (\text{A-1})$$

$$S_n = \sum_{n=k+1}^{\infty} \frac{\cos a a - \cos a b}{n+j} \sin \alpha x = \frac{1}{2} \sum_{i=1}^4 \sum_{n=k+1}^{\infty} \frac{\sin n \beta_i}{n+j} \quad (\text{A-2})$$

in which, β_i has been shown in Eq. (37).

$$\sum_{n=k+1}^{\infty} \frac{\sin n \beta_i}{n+j} = \sum_{n=1}^{\infty} \frac{\sin n \beta_i}{n+j} - \sum_{n=1}^k \frac{\sin n \beta_i}{n+j} \quad (\text{A-3})$$

and

$$\sum_{n=1}^{\infty} \frac{\sin n \beta_i}{n+j} = \sum_{n=1}^{\infty} \frac{\cos j \beta_i \sin(j+n)\beta_i - \sin j \beta_i \cos(j+n)\beta_i}{j+n}$$

but

$$\sum_{n=1}^{\infty} \frac{\sin(j+n)\beta_i}{j+n} = \sum_{n=1}^{\infty} \frac{\sin n \beta_i}{n} - \sum_{n=1}^j \frac{\sin n \beta_i}{n}$$

hence

$$\sum_{n=1}^{\infty} \frac{\sin n \beta_i}{n+j} = \cos j \beta_i \sum_{n=1}^{\infty} \frac{\sin n \beta_i}{n} - \sin j \beta_i \sum_{n=1}^{\infty} \frac{\cos n \beta_i}{n} + \sum_{n=1}^j \frac{\sin(j-n)\beta_i}{n}$$

where the infinite series can be determined from Ref. [2]:

$$\sum_{n=1}^{\infty} \frac{\sin n \beta_i}{n} = \frac{\pi - \beta_i}{2} \quad (0 < \beta_i < 2\pi)$$

$$\sum_{n=1}^{\infty} \frac{\cos n \beta_i}{n} = -\frac{1}{2} \ln 2(1 - \cos \beta_i) \quad (0 < \beta_i < 2\pi)$$

hence

$$\sum_{n=1}^{\infty} \frac{\sin n \beta_i}{n+j} = \frac{\delta_i}{2} [(\pi - |\beta_i|) \cos j \beta_i + \sin j |\beta_i| \ln 2(1 - \cos \beta_i)] + \sum_{n=1}^j \frac{\sin(j-n)\beta_i}{n}$$

Substituting in Eq. (A-3) and (A-2), we can obtain S_n as shown in Eq. (36).